



Revealing the mechanism of the lutein protective function of epicatechin-fructan glycosylated soybean protein isolate

Yunhan Duan^{a,1}, Yanping Cao^a, Lijun Qi^b, Wang Shaojia^{a,*}, Wei Gao^{b,**}

^a Beijing Advanced Innovation Center for Food Nutrition and Human Health (BTBU), School of Food and Health, Beijing Higher Institution Engineering Research Center of Food Additives and Ingredients, Beijing Technology and Business University, Beijing, 100048, China

^b Chenguang Biotech Group Limited Co., Ltd, Handan, 057250, China

ARTICLE INFO

Handling Editor: Yeonhwa Park

Keywords:

Lutein
Epicatechin
7S globulin
11
Molecular docking
Glycosylated soybean protein isolated

ABSTRACT

Lutein possesses various physiological activities but is susceptible to light degradation, thermal degradation, and oxidative degradation. As such, protecting the activity of lutein-based products using natural extracts has become a current research. In this study, lutein was protected by complexing inulin-type fructan (ITF), soybean protein isolate (SPI), and epicatechin (EC), and the protection mechanism of epicatechin-fructan glycosylated soybean protein isolate (EC-GSPI) toward lutein was elucidated comprehensively. The results showed that the addition of EC delayed the degradation of lutein. The results of light stability experiments showed that increased EC significantly enhanced the storage time of the GSPI-Lutein system from 4 to 13 days. Additionally, the effect of EC on glycosylated soybean 7S globulin (G7S) and glycosylated soybean 11S globulin (G11S) was assessed. The light stability of G11S-Lutein and G7S-Lutein after the addition of EC was from G11S > G7S → G7S > G11S. Furthermore, the proteins purified from SPI interacted differently with EC and ITF, with soybean 7S globulin (7S) mainly interacting with EC and soybean 11S globulin (11S) mainly interacting with ITF. EC-GSPI-Lutein exhibited a good protective effect, probably due to the occurrence of hydrothermal Maillard between ITF and 11S, providing a porous structure for lutein storage. At the same time, the binding of EC to 7S significantly enhanced the antioxidant property of the solution and the stability of the protein secondary structure, thereby prolonging the storage time of lutein.

1. Introduction

With the advancements in people's lifestyles, the requirement for healthy food has become imperative. Natural pigments aid attractiveness to foods, among which lutein possesses excellent physiological functions, such as anti-aging, cataract prevention, and anti-cancer (Alves-Rodrigues and Shao, 2004). Lutein is a carotenoid commonly found in various fruits, vegetables, grains, and flowers, with the highest content being extracted from marigolds (*Tagetes erecta* L.) (Xu et al., 2023). Although lutein has excellent physiological functions, it is susceptible to rapid degradation by light, heat and oxides (Aparicio-Ruiz et al., 2011; Mora-Gutierrez et al., 2022). Currently, lutein esters are being widely used to produce lutein-related products due to their stronger antioxidant properties, less susceptibility to oxidation, and higher bioavailability than lutein. Lutein ester, a natural colouring agent

belonging to oxygenated carotenoids, is characterized by the esterification of lutein with fatty acids, such as lauric, myristic, and palmitic acids, and its primary source is marigold chrysanthemum (Garg et al., 1999; Khalil et al., 2012). With the increasing demands of food industries, the antioxidant properties of lutein esters are falling short of production requirements, requiring novel approaches to improve the storage properties of lutein in food production (Gombac et al., 2021).

In recent years, the application of proteins and modified proteins to protect natural pigments has attracted considerable attention from researchers. Qi et al. screened different proteins for lutein ester protection and found that bovine serum proteins had the best protective effect on lutein esters, followed by whey protein isolate (Qi et al., 2021). Gao et al. found that the protective effect of pigmentation could be enhanced by using different protein interactions with cyanidin (Gao et al., 2022). Yi et al. studied the interaction of milk proteins with lutein and found that hydrophobic interaction was the main force, and milk proteins had

* Corresponding author. No.11, Fucheng Road, Beijing 100048E-, China.

** Corresponding author.

E-mail addresses: wangshaojia@btbu.edu.cn (W. Shaojia), gw@ccgb.com.cn (W. Gao).

¹ These authors contributed equally to this work.

Abbreviations

ITF	inulin-type fructan
SPI	soybean protein isolate
EC	epicatechin
EC-GSPI	epicatechin-fructan glycosylated soybean protein isolate
G7S	glycosylated soybean 7S globulin
G11S	glycosylated soybean 11S globulin
7S	soybean 7S globulin
11S	soybean 11S globulin
GTP	Green tea polyphenols
KBr	potassium bromide
UV-vis	ultraviolet-visible
DTNB	5,5'-dithiobis (2-nitrobenzoic acid)
ANS	1-Aniline naphthalene-8- sulfonic acid
OPA	Ortho-Phthal aldehyde
PDI	polydispersity index
FTIR	Fourier transform infrared
SEM	Scanning electron microscopy

antioxidant and prolonged storage effects on lutein (Yi et al., 2016). It is reported that the application of modified proteins to protect natural pigments exerts better results. Modified proteins not only extend the storage time of natural pigments but also improve physical properties such as protein solubility and emulsification (Jiao et al., 2023; Xu et al., 2016). Protecting lutein by modifying proteins with polysaccharides is one of the most popular means of modification (Mora-Gutierrez et al., 2022). Wang et al. performed lutein protection using inulin-type fructan and soybean protein isolate through the hygrothermal Maillard reaction to prolong the survival time of protection on the original basis by more than a factor of two (Wang et al., 2022). However, these studies still don't satisfy the storage time of the product, demanding the exploration of novel approaches to protect lutein.

Currently, natural extracts have emerged as a potential alternative to commonly used preservatives to inhibit food spoilage with high consumer acceptability. So far, many studies have been reported on the conservation of natural colours with high feasibility (Gu et al., 2022). Yan et al. protected lutein by covalently linking dextran and chlorogenic acid to bovine serum protein and adding vitamin E through an emulsion system, which significantly prolonged the storage time of lutein while enhancing its physical and chemical stability (Yan et al., 2020a). However, there are very few protection systems for lutein that are low cost, made from natural extracts, and have a significant protective effect. Green tea (*Camellia sinensis*) polyphenols (GTP) are the primary chemical components of tea, with excellent healthcare functions and various physiological activities (Zhang et al., 2019). Epicatechin (EC) is a tea polyphenol with a more prominent antioxidant and clear free radical ability (Gao et al., 2013). Inulin-type fructan (ITF) has the properties of enhancing body resistance, accelerating metabolism, relieving fatigue, anti-ageing, and antioxidation (Kaur and Gupta, 2004); Additionally, it has the advantages of low cost and ample output, making it more suitable for practical production applications. Soybean protein isolate (SPI), produced under low-temperature conditions by soy (*Glycine max* (L.) Merr.), retains the best soybean ingredients and the rich variety of amino acids and removes the inhibitory protein factor, purine, and other soybean components not beneficial to absorption and health (Song et al., 2011). Additionally, SPI has low costs and high productivity. The 11S globulin present in SPI has the potential to cause allergies. However, the addition of epicatechin can inhibit this reaction (L. Li et al., 2023). Therefore, in this study, soybean protein isolate, inulin-type fructans, and epicatechin were selected as the research materials to protect lutein and reveal its mechanism of action. The protection system's materials consist solely of natural extracts, which are cost-effective and easy to

apply in production. Additionally, this system provides a theoretical basis for the ternary system's natural pigment protection.

2. Material and methods

2.1. Materials

98% Soybean protein isolate (purity $\geq 98\%$, physical state: powder) was purchased from Yuanye Bio-Technology Biotech Co., Ltd. (Shanghai, China), 95% Inulin-type Fructan (purity $\geq 95\%$, physical state: powder) was purchased from ChenGuang Bio-Technology Biotech Co., Ltd. (Hebei, China), Sodium dihydrogen phosphate (purity $\geq 99\%$, physical state: powder) was purchased from fuchen Chemical Biotech Co., Ltd. (Tianjin, China), Sodium Phosphate, Dibasic (purity $\geq 99\%$, physical state: powder) was purchased from fuchen Chemical Biotech Co., Ltd. (Tianjin, China), Tea Polyphenols (purity $\geq 98\%$, physical state: powder) was purchased from MREDA Biological Biotech Co., Ltd. (Beijing, China), Epicatechin (purity $\geq 95\%$, physical state: powder) was purchased from MREDA Biological Biotech Co., Ltd. (Beijing, China), Hydrochloric acid (purity $\geq 36\%$, physical state: fluid) was purchased from MREDA Biological Biotech Co., Ltd. (Beijing, China), Sodium hydroxide (purity $\geq 96\%$, physical state: powder) was purchased from MREDA Biological Biotech Co., Ltd. (Beijing, China), Lutein (purity $\geq 95\%$, physical state: Semi-fluid) was purchased from banxia Biotech Co., Ltd. (Qinghai, China), Micro Total Mercapto Assay Kit (BC1375-100T/48S) was purchased from Solebro Biological Biotech Co., Ltd. (Beijing, China), 12 percent of the separation gel premix was purchased from Solebro Biological Biotech Co., Ltd. (Beijing, China), 5 percent concentrated gum gum premix was purchased from Solebro Biological Biotech Co., Ltd. (Beijing, China), Ammonium persulfate (purity $\geq 99\%$, physical state: powder) was purchased from Solebro Biological Biotech Co., Ltd. (Beijing, China), 2X protein loading buffer was purchased from Solebro Biological Biotech Co., Ltd. (Beijing, China), 1X Tris-Glycine Electrophoresis Buffer was purchased from Solebro Biological Biotech Co., Ltd. (Beijing, China), Rainbow 180 Spectrum Protein Maker was purchased from Solebro Biological Biotech Co., Ltd. (Beijing, China), 8-Aniline-1-naphthalene sulfonic acid (purity $\geq 96\%$, physical state: powder) was purchased from MREDA Biological Biotech Co., Ltd. (Beijing, China).

2.2. Sample preparation

2.2.1. Preparation of 7S globulin and 11S globulin

SPI was mixed with deionized water at a ratio of 1:20 (w/w), and the pH was adjusted to 8.0 with 0.1 mol/L NaOH solution. After stirring at room temperature for 24 h, it was centrifuged at 10,000 $\times g$ for 30 min at 4 °C. Then, the precipitate was removed to leave a supernatant, and anhydrous sodium sulphate was added to adjust the SO_4^{2-} to 0.01 mol/L. Later, 1 mol/L of HCl was added to the supernatant to adjust the pH to 5.8 and left to stand at 4 °C for 12 h. At the end of the standing period, it was centrifuged at 4 °C and 10,000 $\times g$ for 30 min, and the precipitate obtained was soybean 11S globulin. The supernatant of the second centrifugation was adjusted to pH 5.0 with 1 mol/L of HCl and then centrifuged at 10,000 $\times g$ for 30 min at 4 °C. After centrifugation, the precipitate was discarded, and the supernatant was taken and added to an equal volume of deionized water to adjust the pH to 4.5 with 1 mol/L of HCl, followed by centrifugation at 10,000 $\times g$ for 30 min at 4 °C. Finally, the resultant precipitate was soybean 7S globulin (Gao et al., 2016).

2.2.2. glycosylated soybean protein isolate preparation

Approximately 2 g of SPI/7S/11S solid powder and 2g of Inulin-type fructan solid powder were dissolved in a phosphate buffer solution (0.01 mol/L), the pH was adjusted to 11.0 with 0.1 mol/L of NaOH, and finally made up to 100 mL. After full dissolution, the reaction was carried out in boiling water at 100 °C for 4 h and 42 min in a Maillard reaction.

2.2.3. EC-fructan glycosylated soybean protein isolate and lutein complex preparation

Approximately 15 mL of glycosylated protein (GSPI/G7S/G11S) was prepared as mentioned in section 2.2.2, and 50 mL of phosphate buffer solution (0.01 mol/L) with pH = 7 and 1 mL of lutein solution (5 mg/mL) were added. The solution was mixed thoroughly, followed by the addition of 5 mg of EC (purity $\geq 98\%$, physical state: powder), and continuous mixing for half an hour. At the end of mixing, the pH was adjusted to 7 with HCl (0.1 mol/L) and made up to 100 ml with phosphate buffer.

2.3. Light stability

The SPI, 7S and 11S proteins were glycosylated and added to polyphenols for light stability experiments at 25 °C and a 202 nm UV wavelength. After sampling, the samples were tested by a colour difference metre. The CIELAB Tristimulus coordinates (L^* , a^* , b^*), ΔE , and ΔB were obtained. L^* means bright and dark, +means brighter, scale from 0 to 100; a^* means red and green, +means reddish, - means greenish, scale from -128 to +127; b^* means yellow and blue, +means yellowish, - means blueish, scale from -128 to +127. ΔE is the change in the overall colour difference of the substance between the initial and current states. ΔB is the change in the difference between the initial b value and the current b value (Jv et al., 2023). The value ($\Delta E, \Delta B$) were as follows:

$$\Delta B = b^*_0 - b^*$$

$$\Delta E = \sqrt{(\Delta L^*)^2 + (\Delta a^*)^2 + (\Delta b^*)^2}$$

2.4. Fourier transform infrared (FTIR) spectroscopy

SPI, EC-SPI, GSPI, EC-GSPI, G7S, EC-G7S, G11S, EC-G11S, G11S, and EC-G11S were ground into powder by freeze-drying in a freeze-dryer, and then 2–3 mg of the sample powder was taken, ground and mixed with potassium bromide (KBr), extruded to make a transparent sheet, and loaded into a sample rack. The lower panel of the sample holder was adjusted to the proper position and then inserted into the upper panel. It was fixed diagonally with screws and then inserted into the detection cell to measure the sample infrared spectrum. The detection range was 4000–400 cm^{-1} . The secondary structure was then analyzed by fitting the infrared spectrum to 1700–1600 cm^{-1} using PeakFit 4.12 software (Balakhmina et al., 2017).

2.5. Fluorescence spectroscopy

Protein (1 mg/mL) or modified protein (1 mg/mL) was injected into the enzyme labelling plate at 250 μL per well per sample in 6 parallels. The fluorescence emission spectra were measured by a multifunctional enzyme marker (Infinite 200 PRO) at 25 °C. The specific parameters were as follows: the spectral width of excitation and emission was 5 nm, the voltage was 80 V, and the scan speed was 2400 nm/min. The excitation wavelength was set at 280 nm for selective excitation of the three classes of colour-emitting amino acids, and the emission wavelength was specifically observed between 310 nm and 450 nm (Tian et al., 2021).

2.6. Ultraviolet-visible (UV-vis) spectra

SPI, GSPI, EC-SPI, EC-GSPI, G7S, EC-G7S, and EC-G11S were diluted to 3 mg/mL, and the pH was adjusted to 7.0. Then, 10 mm of the quartz sampling cells were rinsed with the samples, and the samples were added after rinsing. The spectra were scanned in the wavelength range of 200–500 nm using a UV-visible spectrophotometer (Agilent Cary 60) at 300 nm/min. The UV spectra were recorded on a computer after scanning (Krebs et al., 2017).

2.7. Total sulfhydryl content and hydrophobicity

DTNB is for the abbreviated form of 5,5'-dithiobis (2-nitrobenzoic acid) (5,5'-dithiobis-(2-nitrobenzoic acid)) (Zheng et al., 2003). The total sulfhydryl content of proteins is mainly detected using the DTNB method. In this experiment, the proteins (1 mg/mL) or covalent proteins (1 mg/mL) were assessed using the total sulfhydryl kit following the manufacturer's instructions (solarbi-BC1370).

The 1-Aniline naphthalene-8-sulfonic acid (ANS) method is a common assay for determining the hydrophobicity of proteins (Alizadeh-Pasdar and Li-Chan, 2000), in which proteins or covalent proteins are dissolved into a phosphate buffer solution of 3 mg/mL at pH = 7.0, and the mass gradient is diluted to 5 gradients from 3 to 0.1875 mg/mL. In this study, 2 mL of the sample solution was added to 20 μL of ANS (8 mmol/L), and then it was shaken and allowed to stand for 3 min. The excitation wavelength was set at 390 nm (slit-corrected 5 nm), and the emission wavelength was set at 470 nm (slit-corrected 5 nm). Finally, the fluorescence intensity was measured. A curve was plotted with the fluorescence intensity against the protein concentration, and the slope of the initial stage of the curve was the hydrophobicity of the protein surface.

2.8. Protein binding properties

2.8.1. Ortho-phthalaldehyde method

The degree of glycation of proteins was determined by measuring the degree of reduction of free amino acids in the SPI and conjugate material using the Ortho-phthalaldehyde (OPA) method. A total of 80 mg of OPA was dissolved in a mixture containing 2 mL of 95% ethanol, 50 mL of tetraborate buffer (0.1 mol/L, pH 9.5), 5 mL of SDS (20% w/v), and 0.2 mL of 2-mercaptoethanol. Later, the mixture was diluted to 100 mL with ultrapure water.

The sample solution of 3 mg/mL protein or covalent complex (containing 3 mg/mL protein) was mixed with OPA reagent at 20:1 (v/v) and incubated for 2 min at 35 °C in a thermostatic incubator. The absorbance value of the solution was measured at 340 nm (Fan et al., 2018).

$$DG (\%) = \frac{[(\text{Absorbance of unglycosylated SPI} - \text{Absorbance of glycosylated SPI}) / \text{absorbance of unsweetened SPI}] \times 100\%}{}$$

2.8.2. Molecular docking

The results of molecular docking of 7S and 11S with epicatechin indicated the molecular docking simulation by cavityPuls. Soybean 11S protein (PDB:1OD5) and soybean 7S protein (PDB:3AUP) were used as the receptor, and the ligand was epicatechin (Song et al., 2023). The docking model was constructed using Chem 3D, and the minimum binding energy was analyzed using PyMOL software. The detailed methodology is described in the supplementary material.

2.9. Scanning electron Microscopy (SEM)

The morphology of eight proteins, including SPI, EC-SPI, GSPI, EC-GSPI, G7S, EC-G7S, G11S, and EC-G11S, as well as covalent proteins, was observed using a scanning electron microscope after freeze-drying. The samples were then spray-painted with sheet metal and observed under a scanning electron microscope (SU1510). Later, the images were captured at a resolution of 1000X and 2000X at 5 KV.

2.10. Particle diameter, polydispersity index (PDI) and ζ -potential

Particle size and zeta potential were measured according to the previously reported method with minor modifications (Huang et al., 2022). The EC-GSPI, EC-SPI, GSPI, SPI, 7S, 11S, G7S, G11S, EC-G7S, and EC-G11S solutions were diluted to 1 mg/mL and the pH was adjusted to

7.0 using phosphate buffer solution (pH = 7.10 mmol) and 0.1 mol/L of HCl. The samples were added to the quartz sampling cell and folded capillary cell, respectively, and the particle size and zeta potential were measured using a particle size analyser (ZEN3690).

2.11. Statistical analysis

Three batches of samples were prepared, and all measurements were performed in triplicate, of which the fluorescence experiments were performed in six replicates. The results were expressed as mean \pm standard deviation. The evaluation and analysis were performed using SPSS software. Significant differences between the means were analyzed by one-way analysis of ANOVA ($P < 0.05$) and independent samples *t*-test (T) ($P < 0.05$).

3. Results and discussion

3.1. Light stability

Chromatic aberration is the most intuitive indicator of colour change. Since the primary colour of lutein is yellow, b^* and ΔE can characterize the colour changes in the solution system. As shown in Fig. 1a, the b^* value of SPI-lutein was 5.24 after 24 h of UV irradiation, while the b^* value of GSPI-lutein reached this level after 144 h of UV irradiation. Meanwhile, the b^* value of EC-GSPI-lutein was still 11.14 after 144 h of UV irradiation following the addition of EC. This result suggests that glycosylation could protect the proteins from lutein light degradation, and the addition of EC could significantly extend this protection time. The modification to EC-GSPI-lutein extended the protection time of SPI-lutein from 24 h to 336 h. Li et al. found that the application of glycosylated proteins to protect proanthocyanidins improved the stability of the pigments (Y. Li et al., 2023; Yan et al., 2020b). As shown in Fig. 1a, the b^* value of the purified protein G7S-lutein was lower than that of G11S-lutein. However, after EC addition, the b^* value of EC-G11S-lutein was lower than that of EC-G7S-lutein. This indicates that different modification behaviors have varying effects on different proteins. ΔE showed a similar trend (Fig. 1b).

Typically, the addition of polyphenols leads to changes in protein structure, and polysaccharides form complexes with proteins through a hydrothermal Maillard reaction, both of which increase the antioxidant properties of the system. This improvement leads to increased protective effects of lutein, with glycosylated soybean protein isolate shielding it

primarily through hydrophobic cavities (Wang et al., 2022). The results of the light stabilization experiments indicate that both EC and glycosylation reactions could enhance the protective effect of lutein in this system by altering the protein structure. Therefore, assessing the structural modification of SPI and its isolated products through EC and glycosylation reactions is crucial for studying this protective mechanism.

3.2. Fourier transform infrared (FTIR) spectroscopy analysis

Fourier infrared (FTIR) spectroscopy is commonly used to analyse the changes in the structure of the functional groups of substances and the secondary structure of proteins. The secondary structure was characterized by fitting the infrared spectrum 1600-1700 cm^{-1} to the analysis, as shown in Table 1. The β -fold is an ordered structure in the protein structure, and its content can reflect the stability of the protein. In this study, the addition of EC enhanced the β -folding content, with SPI being the most obvious, and the glycosylated protein had a certain degree of enhancement (Yan et al., 2020a). Glycosylated G11S had a more ordered and stable structure than G7S, and G7S had a higher content of β -turns, indicating better emulsification. Therefore, it can be concluded that the improvement in SPI stability by glycosylation mainly affects soybean 11S globulin. Both EC and glycosylation can improve the stability and antioxidant capacity of proteins, which is beneficial for loading lutein to extend its shelf life (Liu et al., 2023). In this study, EC-GSPI, EC-G11S, and EC-G7S had higher β -folding content than GSPI, G11S, and G7S, indicating that the ternary complexes are more stable and more conducive to lutein protection (Chen et al., 2021).

The addition of EC induced vibration in the SPI at 3352 cm^{-1} and its

Table 1

Proportion of protein secondary structures of SPI, EC-SPI, GSPI, EC-GSPI, G7S, EC-G7S, G11S and EC-G11S.

name/Secondary structure	β -folding (%)	curl up irregularly (%)	α -Spiral (%)	β -turn (%)
EC-G7S	21.8	18.0	20.5	39.7
G7S	21.6	18.3	20.6	39.5
EC-G11S	25.8	18.2	19.1	36.8
G11S	25.5	18.3	19.2	36.9
EC-GSPI	25.2	18.2	19.3	37.2
GSPI	25.1	18.5	19.5	36.9
EC-SPI	22.9	18.0	20.5	38.4
SPI	19.4	17.9	20.9	41.7

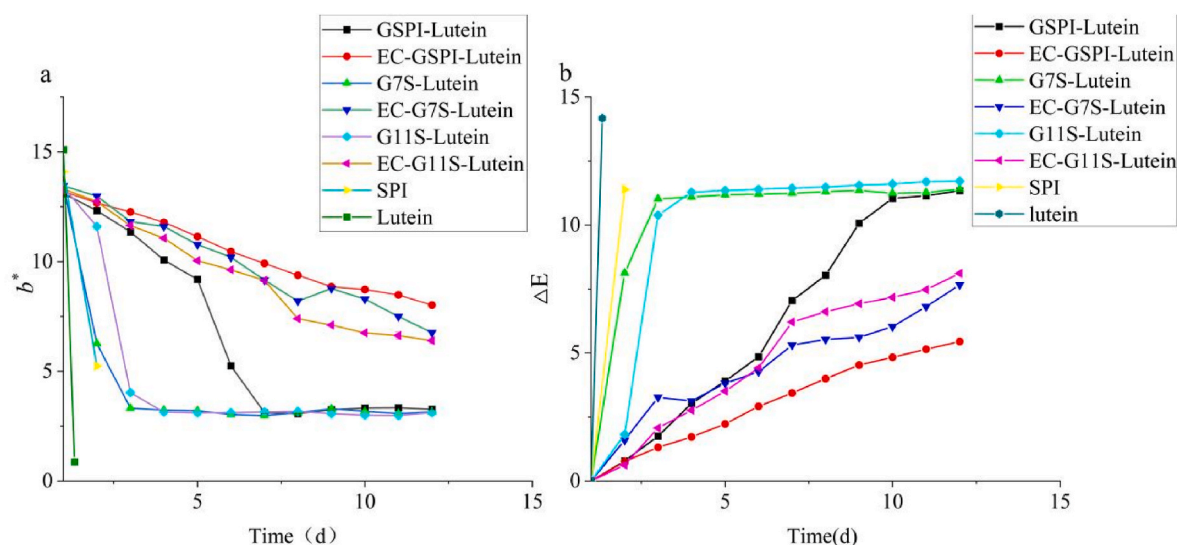


Fig. 1. (a) Effect of EC on different glycosylated protein-lutein complexes (b^*), (b) Effect of EC on different glycosylated protein-lutein complexes (ΔE).

peak intensity increased significantly. This result indicates that the molecular hydrogen bonds between the carboxyl group and the amino group could vibrationally stretch each other, and EC is mainly bonded to SPI by hydrogen bonding (Zhou et al., 2023). As shown in Fig. 2 a and b, the addition of EC affected the structure of $-CH_2$ in SPI and glycosylated proteins, producing a significant shift near 2930 cm^{-1} . This might be due to the symmetric stretching vibration of $-CH_2$, indicating the appearance of carbon-hydrogen bond formation, which was consistent with the molecular docking results. At approximately 2900 cm^{-1} , the peak positions of the SPI with and without EC showed some changes, suggesting that hydrophobicity occurs during the coupling of proteins to the polyphenols (Su et al., 2020); This might be attributed to the fact that the polyphenols induce protein aggregation, which prevents the formation of hydrophobic forces between the polyphenols and the hydrophobic groups inside the protein, leading to a decrease in the hydrophobic effect (Mohammadi et al., 2023).

3.3. Fluorescence spectroscopy analysis

Fluorescence spectroscopy is widely used to determine the protein tertiary structure. After certain degrees of changes in the structure and fluorescence, Proteins the proteins in the glycosylation and polyphenol graft after the structure of different degrees of change and fluorescence can be reflected from the interaction between different individuals. In such cases, the chromogenic group tryptophan is the main contributor to the intrinsic fluorescence of proteins, along with tyrosine and phenylalanine, which also have a chromogenic function. As shown in Fig. 3 a, the fluorescence intensity of SPI was significantly reduced and redshifted after glycosylation, indicating that protein glycosylation reduces hydrophobicity and increases the degree of protein stretching. The decrease in the fluorescence intensity might be attributed to the masking of chromophores in SPI by the glycosylation process (Huang et al., 2023). As for the three glycosylated proteins, G7S, G11S, and GSPI, the addition of EC caused the glycosylated proteins to blueshift, increased the hydrophobicity and macromolecules in the folded state stability, and decreased the α -helix. This result suggests that EC could enhance the stability of glycosylated proteins and facilitate the loading of glycosylated proteins with lutein to prolong their storage time (Moller and Denicola, 2002). Generally, the fluorescence intensity of polyphenols covalently bound to proteins decreases due to the masking of the chromophores. However, in this study, the fluorescence intensity

increased, probably due to the interference of the aromatic groups in the EC itself, which were similar to the aromatic amino acids at approximately 280 nm (Fig. 3 b). It can be seen that the fluorescence intensity of EC exceeded the detection limit at 80 V , indicating that the fluorescence intensity of EC decreased after binding to the protein.

3.4. UV-Vis absorption analysis

UV spectroscopy is a promising method for studying the internal structure of biological macromolecules and analyse the absorption peaks produced by solution samples in different wavelength bands. The light absorption of proteins in the ultraviolet region ($250\text{--}300\text{ nm}$) is mainly due to the electronic excitation of the aromatic amino acids Trp and Tyr and, to a lesser extent, Phe and His (Sonu et al., 2017). As shown in Fig. 4 a, the addition of EC caused a blueshift of the maximum absorption peak of the protein, thereby increasing the glycosylation protein conjugation system and the spatial resistance of the soybean protein isolates and altering the conjugation system protein structure. As shown in Fig. 4 c, EC caused redshifts of G7S and G11S, probably due to the introduction of the $-OH$ electronic groups by the addition of EC. The degree of covalency can be explained by the intensity of its peaks in each group through $EC\text{-G11S} > EC\text{-G7S} = EC\text{-GSPI} > G11S > G7S = GSPI > EC\text{-SPI} > SPI$ (Fig. 4). This result indicates that the main provider of covalency degree is glycosylation or the hydrothermal Maillard reaction, followed by the addition of EC (Zhao et al., 2020). Overall, 11S glycosylation was more effective and obvious, and the addition of EC improved a part of the covalent degree, increasing the covalent intensity of EC-G11S.

3.5. Total sulfhydryl content and hydrophobicity

The hydrophobicity of proteins is the tendency of water to repel nonpolar molecules or groups to interact with each other in water (Chong and Ham, 2014). The total sulfhydryl content is commonly used as an indicator of antioxidant properties and changes in the secondary structure of proteins (Cheng et al., 2022). As shown in Fig. 5 a, both glycosylation and EC increased the total sulfhydryl content: total sulfhydryl content $SPI < GSPI < EC\text{-SPI} = EC\text{-GSPI}$. Glycosylation was more pronounced for G11S sulfhydryl changes, whereas EC was more pronounced for G7S sulfhydryl changes, suggesting that different modification methods have different effects on different soybean globulins. This might be due to the fact that 7S protein binding to EC is mainly

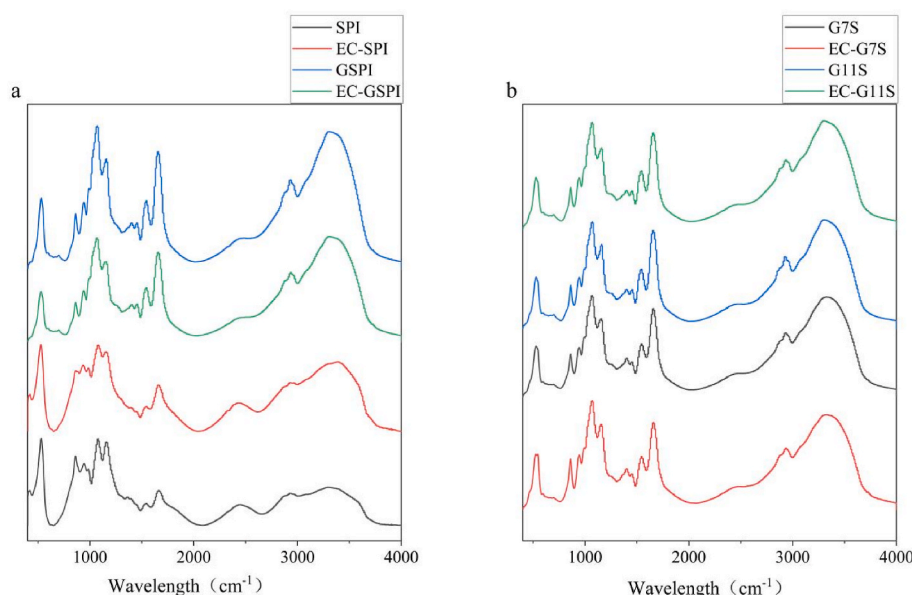


Fig. 2. (a) Effect of EC on the infrared spectra of SPI and GSPI, (b) Effect of EC on the infrared spectra of G7S and G11S.

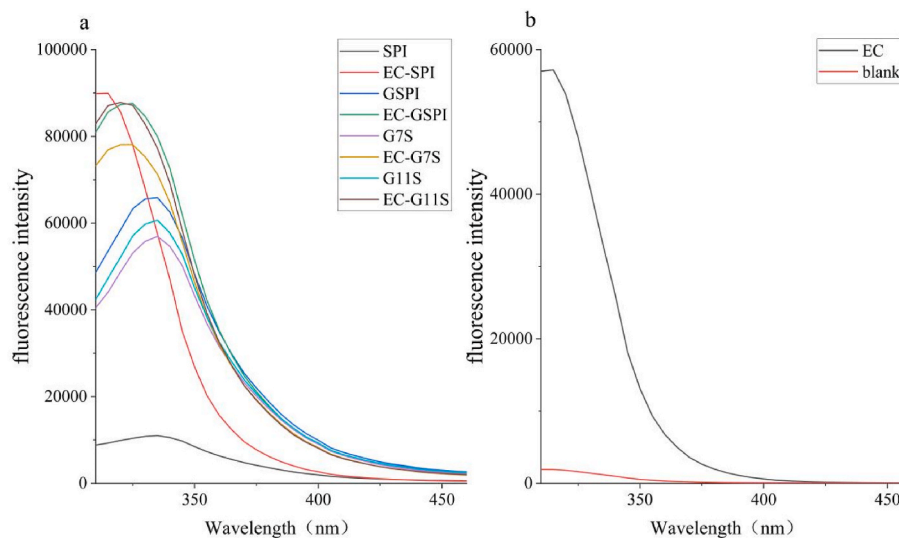


Fig. 3. (a)Effect of EC on the fluorescence emission spectra of SPI, GSPI, G7S, and G11S,(b)Fluorescence emission spectra of EC and blank groups.

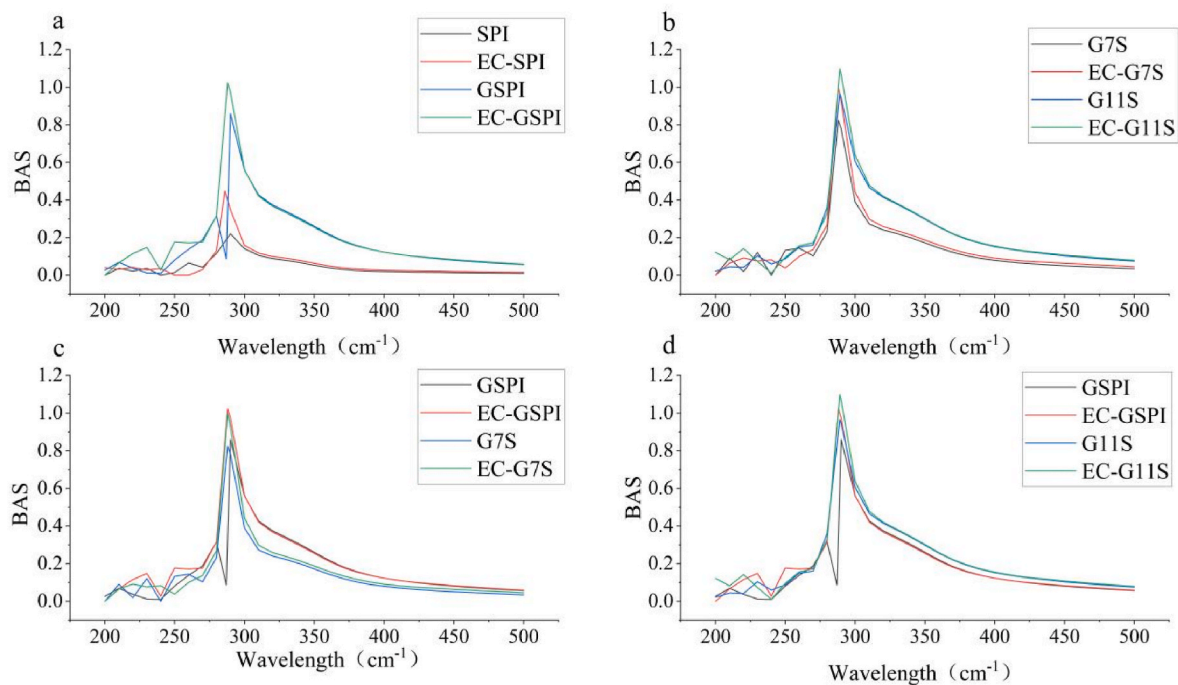


Fig. 4. (a)Comparison of the UV spectra of EC to SPI and GSPI,(b)Comparison of the UV spectra of EC to G7S and G11S,(c)Comparison of the UV spectra of EC to G7S and GSPI,(d)Comparison of the UV spectra of EC to G11S and GSPI.

based on hydrophobic bonding, whereas 11S binding to EC is mainly hydrogen bonding and van der Waals forces, and the number of its conventional hydrogen bonds between 11S and inulin is greater than the number of conventional hydrogen bonds between 7S and inulin. As shown in Fig. 5 b, the addition of EC resulted in proteins producing different degrees of hydrophobicity reduction, with EC addition having the strongest effect on G7S, leading to a significant reduction in its hydrophobicity. This result was consistent with the findings of binding strength of the total sulfhydryl content.

3.6. Protein binding properties

3.6.1. Degree of covalency

The grafting degree is one of the most common metrics used to

evaluate modified proteins, reflecting the extent to which the protein binds to other compounds. As shown in Fig. 6 a, the degree of glycosylation of GSPI was only 10.5%, whereas the degree of glycosylation of G11S and G7S reached 219.1% and 80.1%, respectively. This finding indicated that purified proteins were significantly more glycosylated than unpurified glycosylated proteins, and 11S proteins were more readily covalent with ITF than 7S proteins. Meanwhile, the degree of grafting of GSPI and EC-GSPI was 10.5% and 9.9%, respectively, indicating that the degree of glycosylation of glycosylated proteins decreased to some extent after the addition of polyphenols. This is probably because EC occupies some of the free amino acid sites of SPI, and EC reacts with SPI to form oxidized quinone (Fan et al., 2018). As shown in Fig. 6 b, free amino acids were the lowest in 11S protein and the highest in 7S, suggesting that the grafting of 11S protein with ITF

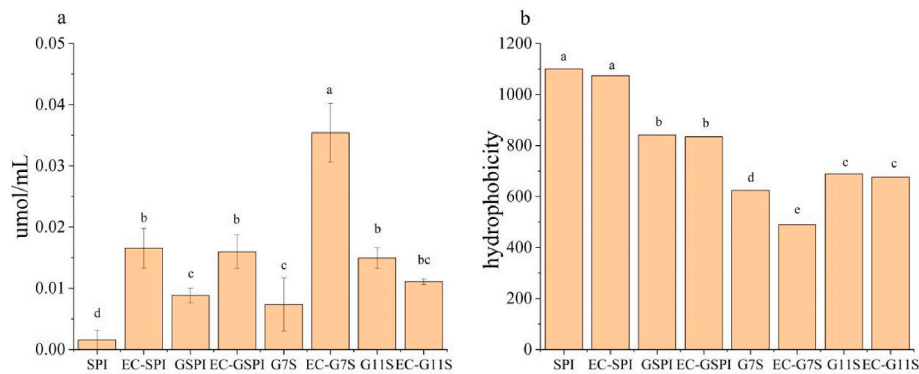


Fig. 5. (a)Effect of EC on the total sulfhydryl content of different proteins and different glycosylated proteins,(b)Effect of EC on the hydrophobicity of different proteins and different glycosylated proteins.

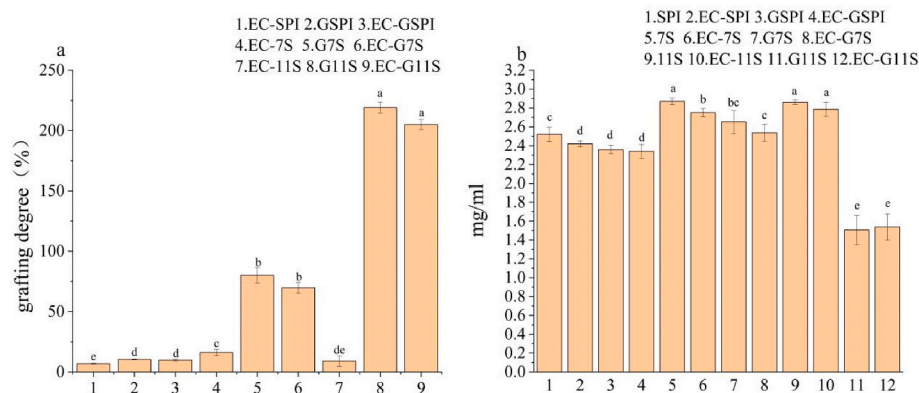


Fig. 6. (a)Grafting degree of SPI, EC-SPI, GSPI, EC-GSPI, EC-7S, G7S, EC-G7S, EC-11S, G11S, EC-G11S,(b)Free amino acid content of SPI, EC-SPI, GSPI, EC-GSPI, EC-7S, G7S, EC-G7S, EC-11S, G11S, EC-G11S.

was better than other proteins.

3.6.2. 2Molecular docking

The docking of 7S and 11S proteins was modelled with inulin and EC using a molecular docking technique. This type of computational analysis highlights the position with the best affinity for non-covalent bonds. The results showed that the docking scores of 7S and 11S proteins with EC were 8.91 and 8.77, respectively, whereas their docking scores with inulin were 10.78 for 11S protein and 8.08 for 7S protein. It can be seen from the binding scores that the 7S protein binds more strongly to EC than 11S, while 11S binds more strongly to inulin than 7S, illustrating the different functional contributions of different proteins in the EC-GSPI. Additionally, this finding explains the higher degree of glycosylation of 11S with inulin than that of 7S, supporting the different effects of EC on 7S and 11S.

3.6.2.1. 11S molecular docking. The main interaction forces between EC and 11S are hydrogen bonding (Fig. 7), electrostatic, and van der Waals forces. The benzene group of epicatechin formed one Pi-donor hydrogen bond interaction with Ser487 in chain F of soybean 11S globulin. The benzene groups of epicatechin formed two electrostatic interactions with Glu87 in chain E and Glu87 in chain D of soybean 11S globulin. Three oxygen atoms of epicatechin, regarded as hydrogen bond acceptors, formed three conventional hydrogen bond interactions with Glu87 in chain D and Ser110 and Gly321 in chain E of soybean 11S globulin. Two oxygen atoms of epicatechin, regarded as hydrogen bond donors, formed two conventional hydrogen bond interactions with Glu87 in chain E and Gly321 in chain D of soybean 11S globulin. Moreover, van der Waals interactions were observed between epicatechin and soybean 11S globulin.

The interaction forces between 11S and fructose are mainly hydrogen bonding, carbon-hydrogen bonding, and van der Waals forces. Hydrogen bonds and van der Waals (VDW) interactions were formed between inulin and soybean 11S globulin. Six oxygen atoms of inulin, regarded as hydrogen bond acceptors, formed six conventional hydrogen bonds with Asn486 and Ser487 in the chain C, Gln108 in the chain D, Gly485 and Ser487 in the chain F of soybean 11S globulin (Fig. 8). Seven oxygen atoms of inulin, regarded as hydrogen bond donors, formed seven conventional hydrogen bonds with Tyr483 and Ser487 in the chain C, Gln108 in the chain D, Glu87 in the chain E, Ser487 and Asp457 in the chain F of soybean 11S globulin. One oxygen atom of inulin, regarded as hydrogen bond acceptor, formed one carbon hydrogen bond with Pro86 in the chain E of soybean 11S globulin. van der Waals interactions were also formed between inulin with soybean 11S globulin. These interactions mainly contributed to the binding energy between inulin and soybean 11S globulin.

3.6.2.2. 7S molecular docking. The predicted binding mode of epicatechin with soybean 7S globulin is illustrated in Fig. 9. As shown in Fig. 9, hydrogen bond, hydrophobic, and van der Waals (vdW) interactions were formed between epicatechin and soybean 7S globulin. The benzene group of epicatechin formed one Pi-Donor hydrogen bond interaction with Thr223 in the chain B of soybean 7S globulin. Two oxygen atoms of epicatechin, regarded as hydrogen bond donors, formed two conventional hydrogen bond interactions with Asn231 in the chain B and Val255 in the chain D of soybean 7S globulin. Moreover, hydrophobic interactions were observed between epicatechin and Pro221, Arg233 in the chain B of soybean 7S globulin.

The predicted binding mode of inulin with soybean 7S globulin was illustrated in Fig. 10. The inulin formed a suitable steric

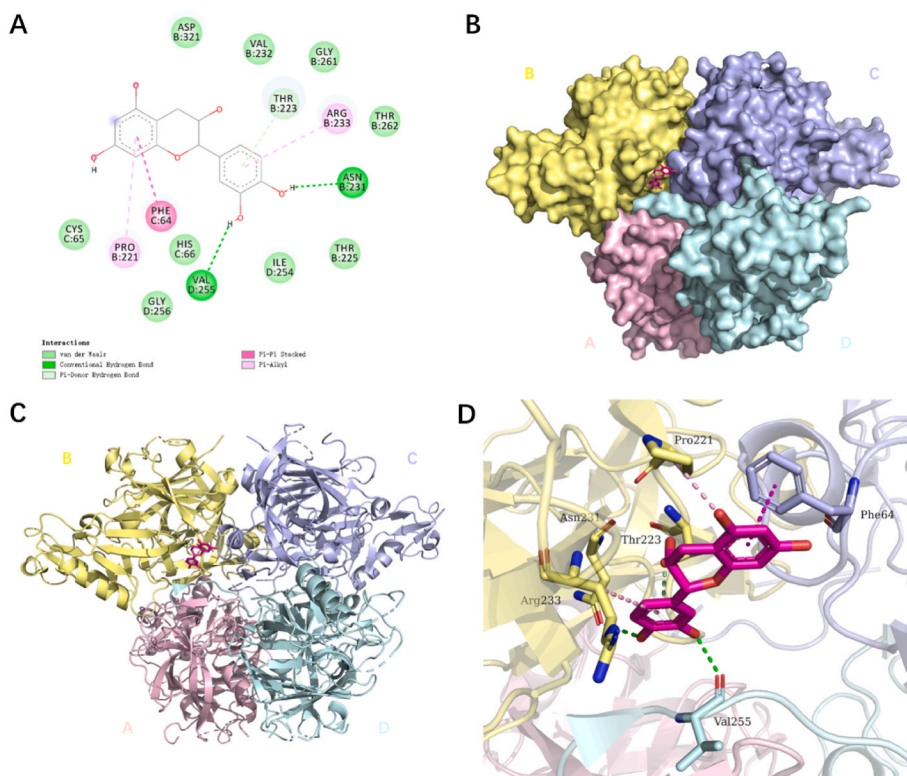


Fig. 9. (A) The 2D binding mode of epicatechin and soybean protein 7S,(B)The 3D-surface binding mode of epicatechin and soybean protein 7S,(C)The 3D-label binding mode of epicatechin and soybean protein 7S,(D)The 3D-detail binding mode of epicatechin and soybean protein 7S..(For an explanation of the legend, please see the supplementary material.)

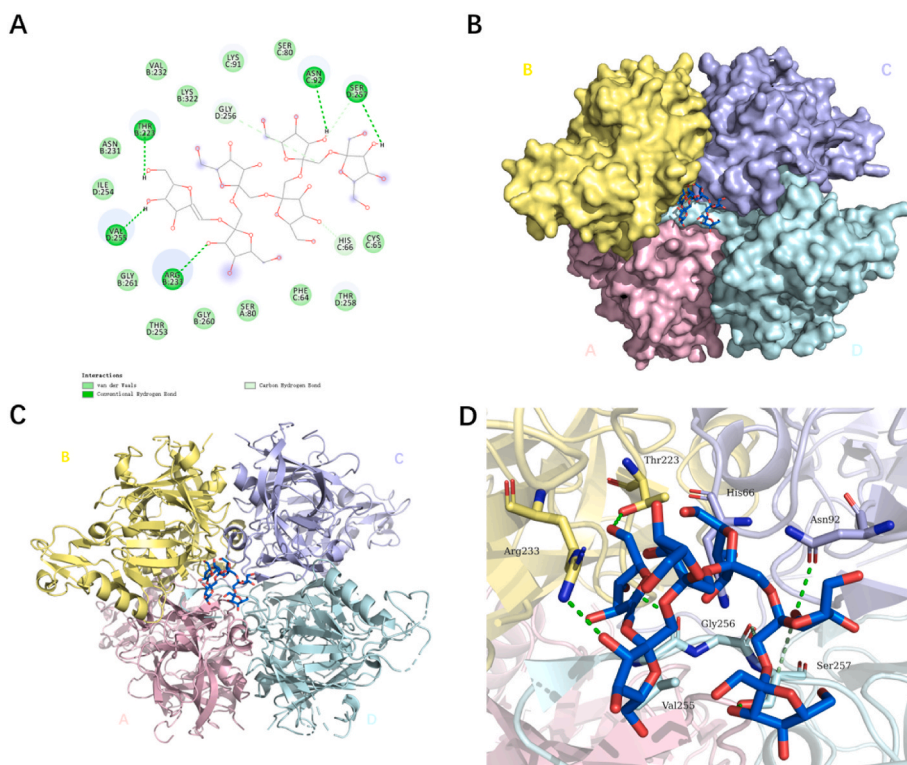


Fig. 10. (A)The 2D binding mode of inulin and soybean 7S protein,(B)The 3D-surface binding mode of inulin and soybean 7S protein,(C)The 3D-label binding mode of mode of inulin and soybean 7S protein, (D)The 3D-detail binding mode of mode of inulin and soybean 7S protein..(For an explanation of the legend, please see the supplementary material.)

complementarity with the binding site of soybean 7S globulin. Hydrogen bonds and van der Waals (VDW) interactions were formed between inulin and soybean 7S globulin. Four oxygen atoms of inulin, regarded as hydrogen bond donors, formed four conventional hydrogen bonds with Thr223 in the chain B, Asn92 in the chain C, Ser257 and Val255 in the chain D of soybean 7S protein. One oxygen atom of inulin, regarded as hydrogen bond acceptor, formed one conventional hydrogen bond with Arg233 in the chain B of soybean 7S globulin. One carbon atom of inulin, regarded as hydrogen bond donor, formed one carbon hydrogen bond with Gly256 in the chain D of soybean 7S globulin. Two oxygen atoms of inulin, regarded as hydrogen acceptors, formed two carbon hydrogen bonds with His66 in the chain C and Ser257 in the chain D of soybean 7S globulin. van der Waals interactions were also formed between inulin with soybean 7S globulin. These interactions mainly contributed to the binding energy between inulin and soybean 7S globulin.

The comparative analysis between 7S and 11S to EC binding showed hydrophobic interactions between EC and Pro221 and Arg233 in the 7S protein chain B in EC-7S. The hydrophobic force is the stronger form of non-covalent bonds, so 7S was bound more tightly to EC. The comparative analysis between the simulated structures of inulin docked to 7S and 11S showed that 11S linked to inulin possessed one carbon-hydrogen bond with thirteen conventional hydrogen bonds, and 7S linked to inulin possessed three carbon-hydrogen bonds with five conventional hydrogen bonds. The stability of the conventional hydrogen bond is greater than that of the hydrogen bond formed with a carbon atom as a donor. And the reason for this connection is that compared the cysteines in the molecular models of 11S globin and 7S globin. In 11S globulin (PDB ID 1OD5), we observed four cysteine residues forming disulfide bonds or flavonoids using Avogadro, whereas in 7S globulin (PDB ID 3AUP), we directly observed free cysteine residues using Avogadro. The 7S proteins had fewer exposed disulfide bridges compared to the 11S proteins. The exposed thiols in 7S proteins are more favorable for binding to EC, which results in a tighter binding of EC to 7S proteins in molecular docking (Mori et al., 2010). In addition, the Protein-sol patch software analysis revealed that the surface polarity of 11S globular proteins was significantly higher than that of 7S globular proteins. Research indicates that proteins with high surface polarity are more hydrophilic and have stronger hydrogen bonding forces than those with low surface polarity. The primary binding force between inulin and

globulin is hydrogen bonding, which explains why inulin binds more strongly to 11S globulin (Durell and Ben-Naim, 2017). The inulin binds more strongly to 11S globulin, indicating that the 7S and 11S proteins had different functions in the ternary system, where the 7S protein was mainly attached to EC while 11S was mainly attached to inulin. This might explain the results of the photostability and grafting degree experiments.

3.7. Scanning electron microscopy analysis

Scanning electron microscopy (SEM) is a commonly used technique to study protein structure. As shown in Fig. 11, the three unmodified proteins, SPI, 11S, and 7S, showed irregular morphology, with 7S globulin particles being smaller. Upon addition of EC, the surfaces of SPI, 11S, and 7S became smooth and dense (Wen et al., 2014). In the glycosylated proteins G7S, G11S, GSPI, G11S and GSPI showed a loose and porous structure, which was favorable for lutein protection, while G7S showed a dense and smooth lamellar structure. Overall, the addition of EC resulted in smooth and dense structural changes on the surface of glycosylated proteins. The glycosylated proteins associated with GSPI and G11S showed porous structures, whereas G7S was predominantly smooth and lamellar. Therefore, it can be suspected that G11S is the source of the porous structure in GSPI. Overall, the loose and porous ordered structure could make the system more stable and prolong the storage time of lutein. Meanwhile, EC could make the pores smaller and smoother to delay the degradation of lutein.

3.8. Particle diameter, polydispersity index (PDI) and ζ -potential analysis

Particle size and zeta potential are two important indicators for measuring the size of protein particles and the strength of interparticle attraction or particle stability and are commonly used in protein solution systems (Daubert et al., 2006). As shown in Table 2, the particle size and PDI of SPI decreased by 21.5%–79.8% with the addition of EC and glycosylation, while the absolute value of zeta potential increased by 58.2%–275.2%. This indicated that the addition of EC and glycosylation decreased the particle size of SPI and made the system more stable than that of the previous SPI. The particle size of G7S and EC-G7S increased after 7S modification, and the solution homogeneity deteriorated, but its

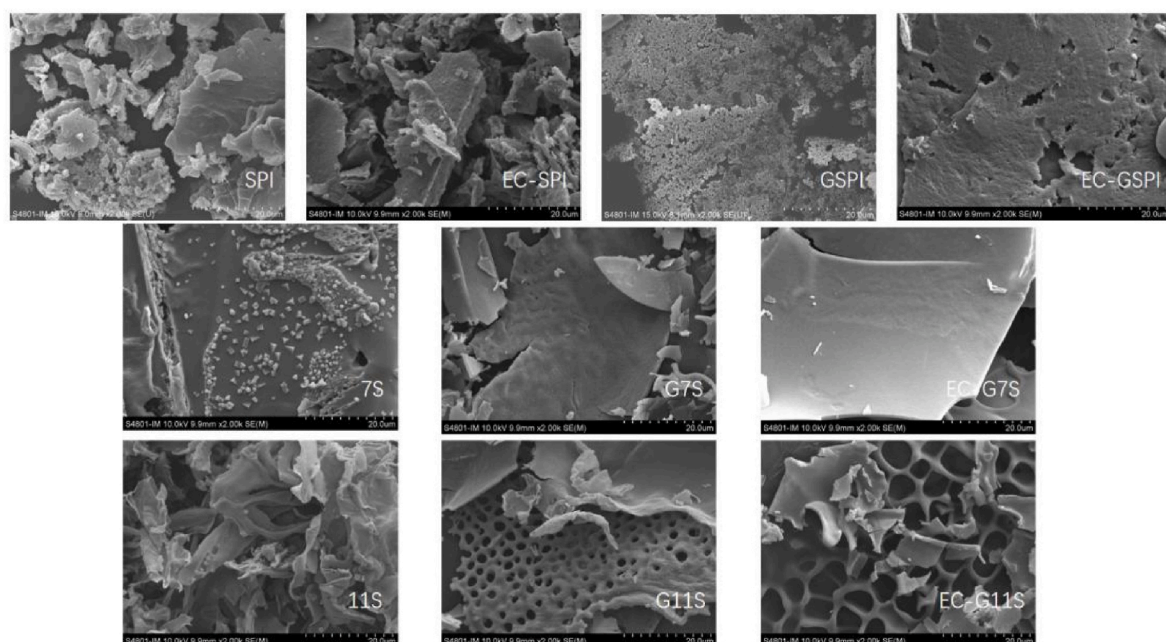


Fig. 11. Sem images of SPI, EC-SPI, GSPI, EC-GSPI, 11S, 7S, G7S, EC-G7S, G11S, EC-G11S.

Table 2

Particle size, PDI, and zeta potential of SPI, EC-SPI, GSPI, EC-GSPI, 7S, 11S, EC-7S, EC-11S, G7S, EC-G7S, G11S, EC-G11S, EC-G11S.

name	Size(nm)	PDI	ZETA(mV)	name	size(nm)	PDI	ZETA(mV)
SPI	925.000 ± 89.632	0.690 ± 0.103	6.181 ± 1.284	EC-SPI	547.000 ± 17.001	0.541 ± 0.157	9.780 ± 1.572
GSPI	188.110 ± 2.003	0.310 ± 0.048	23.190 ± 0.631	EC-GSPI	176.600 ± 2.091	0.324 ± 0.019	24.210 ± 1.376
7S	44.740 ± 13.561	0.410 ± 0.127	14.700 ± 0.882	EC-7S	100.400 ± 5.444	0.333 ± 0.026	15.720 ± 0.954
G7S	443.100 ± 74.031	0.630 ± 0.015	23.481 ± 1.545	EC-G7S	633.200 ± 120.365	0.820 ± 0.052	24.310 ± 0.663
11S	308.300 ± 3.444	0.280 ± 0.005	22.300 ± 0.300	EC-11S	304.110 ± 6.242	0.260 ± 0.014	22.840 ± 0.920
G11S	54.741 ± 21.890	0.590 ± 0.284	21.410 ± 2.010	EC-G11S	52.871 ± 4.756	0.900 ± 0.052	22.790 ± 1.870

inter-particle attraction increased the stability of the solution. Meanwhile, the particle size of 11S became 82.8% smaller, and the PDI value decreased after the addition of EC and glycosylation and the increase in zeta potential increased the aggregation strength and stability. After the ternary conjugation process, the particle size of SPI was stabilized, and the PDI was lowered, indicating that the solution system was more homogeneous and the intermolecular attraction was profound, which is very conducive to the loading of lutein for storage.

4. Conclusions

In this study, the storage time of lutein was prolonged using the natural extracts SPI, ITF, and EC, and their protective mechanisms for lutein were studied. The results showed that the glycosylation of SPI enhanced the protection of lutein, with the addition of EC showing more enhanced protection. The addition of EC and glycosylation retarded the photodegradation of lutein by altering the protein structure. EC increased the ordered structure of SPI, improved the stability, homogeneity, and antioxidant properties of the solution, and prolonged the storage time of lutein. The glycosylation reaction led to the formation of a dense and porous ordered structure of SPI, which increased the β -folding content in the secondary structure and promoted the stability of EC-GSPI-Lutein. Subsequently, the combination of EC, ITF, and SPI significantly prolonged the storage time of lutein.

Additionally, the effect of EC on G7S and G11S was investigated. The protective effect of G7S and G11S on lutein in the presence of EC was $G11S > G7S \rightarrow G7S > G11S$. The results showed that the purified proteins in SPI interacted differently with EC and ITF. Therefore, it was concluded that 7S must be used in conjunction with 11S to maximize the protective effect of EC-glycosylated protein combination. 11S globulin was strongly bound to ITF, while 7S globulin was strongly bound to EC. They played different roles in this ternary system of SPI, EC, and ITF, and the result of this difference in the degree of binding might be due to the fact that the number of conventional hydrogen bonds in the linkage bond between 11S and ITF is greater than that of 7S, and the linkage bond between 7S and EC possesses hydrophobic forces as a strong non-covalent bond. In conclusion, this study has investigated the mechanism of the ternary system to extend the storage time of lutein from a new perspective, which may provides some theoretical basis for the practical delivery of lutein in beverage systems.

CRedit authorship contribution statement

Yunhan Duan: Writing – review & editing, Methodology, Writing – original draft. **Yanping Cao:** Validation, Project administration. **Lijun Qi:** Formal analysis, helped perform the analysis with constructive discussions. **Wang Shaojia:** Conceptualization, Project administration, Supervision. **Wei Gao:** Funding acquisition.

Declaration of Generative AI and AI-assisted technologies in the writing process

Statement: During the preparation of this work the author(s) used artificial intelligence (Microsoft Edge Copilot) in order to language and readability. After using this tool/service, the author(s) reviewed and

edited the content as needed and take(s) full responsibility for the content of the publication.

Declaration of competing interest

The authors declare that they have no known competing financial interests or personal relationships that could have appeared to influence the work reported in this paper.

Data availability

Data will be made available on request.

Acknowledgements

This research was supported by the National Natural Science Foundation of China (31871808), School Level Cultivation Fund of Beijing Technology and Business University for Distinguished and Excellent Young Scholars (BTBUY2020) and Cultivation and Development of Innovation Base (Z171100002217019).

Appendix A. Supplementary data

Supplementary data to this article can be found online at <https://doi.org/10.1016/j.crf.2024.100750>.

References

- Alizadeh-Pasdar, N., Li-Chan, E., 2000. Comparison of protein surface hydrophobicity measured at various pH values using three different fluorescent probes. *J. Agric. Food Chem.* 48 (2), 328–334.
- Alves-Rodrigues, A., Shao, A., 2004. The science behind lutein. *Toxicol. Lett.* 150 (1), 57–83.
- Aparicio-Ruiz, R., Minguez-Mosquera, M.I., Gandul-Rojas, B., 2011. Thermal degradation kinetics of lutein, beta-carotene and beta-cryptoxanthin in virgin olive oils. *J. Food Compos. Anal.* 24 (6), 811–820.
- Balakhnina, I.A., Brandt, N.N., Chikishev, A.Y., Mankova, A.A., Shpachenko, I.G., 2017. Low-frequency vibrational spectroscopy of proteins with different secondary structures. *J. Biomed. Opt.* 22 (9).
- Chen, C., Shi, K., Qin, X., Zhang, H., Chen, H., Hayes, D.G., Wu, Q., Hu, Z., Liu, G., 2021. Effect of interactions between glycosylated protein and tannic acid on the physicochemical stability of pickering emulsions. *Lwt-Food Science and Technology* 152.
- Cheng, J., Sun, J., Yao, K., Xu, M., Zhou, X., 2022. Nondestructive detection and visualization of protein oxidation degree of frozen-thawed pork using fluorescence hyperspectral imaging. *Meat Sci.* 194.
- Chong, S., Ham, S., 2014. Site-directed analysis on protein hydrophobicity. *J. Comput. Chem.* 35 (18), 1364–1370.
- Daubert, C.R., Hudson, H.M., Foegeding, E.A., Prabhasankar, P., 2006. Rheological characterization and electrokinetic phenomena of charged whey protein dispersions of defined sizes. *Lwt-Food Science and Technology* 39 (3), 206–215.
- Durell, S.R., Ben-Naim, A., 2017. Hydrophobic-hydrophilic forces in protein folding. *Biopolymers* 107 (8).
- Fan, Y., Yi, J., Zhang, Y., Yokoyama, W., 2018. Fabrication of curcumin-loaded bovine serum albumin (bsa)-dextran nanoparticles and the cellular antioxidant activity. *Food Chem.* 239, 1210–1218.
- Gao, N., Tian, J., Shu, C., Tan, H., Jiao, X., Lang, Y., Zang, Z., Cui, H., Li, B., 2022. Protective effects and mechanism of amino acids as chokeberry cyanidin and its glycoside protectant under the condition of vitamin c coexistence. *Food Chem.* 397.
- Gao, X., Chen, F., Zhang, L., Bu, G., Fan, M., 2016. Comparison of two soy globulins on the dynamic-mechanical properties of the dough and the quality of steamed bread. *J. Chem.* 2016.

- Gao, Z., Pan, Y., Qin, A., Kang, X., Li, X., Jia, Y., Chen, C., Cui, T., 2013. Synthesis of oil-soluble aliphatic acylated epicatechin and their free radical scavenging activity. *ADVANCES IN CHEMICAL ENGINEERING III* 781–784 (PTS 1–4), 1424–1429.
- Garg, S.N., Charles, R., Kumar, S., 1999. A new acyclic monoterpene glucoside from the capitula of *tagetes patula*. *Fitoterapia* 70 (5), 472–474.
- Gombac, Z., Crnivec, I.G.O., Skrt, M., Istenic, K., Knafelj, A.K., Pravst, I., Ulrih, N.P., 2021. Stabilisation of lutein and lutein esters with polyoxyethylene sorbitan monooleate, medium-chain triglyceride oil and lecithin. *Foods* 10 (3).
- Gu, L., Yao, X., McClements, D.J., Liang, L., Xiong, W., Li, J., Chang, C., Su, Y., Yang, Y., 2022. Lutein-loaded emulsions stabilized by egg white protein-dextran-catechin conjugates: cytotoxicity, stability, and bioaccessibility. *Food Biophys.*
- Huang, P., Wang, Z., Feng, X., Kan, J., 2022. Promotion of fishy odor release by phenolic compounds through interactions with myofibrillar protein. *Food Chem.* 387, 132852.
- Huang, X., Tu, R., Song, H., Dong, K., Geng, F., Chen, L., Huang, Q., Wu, Y., 2023. Fabrication and characterization of gelatin-egg-c-pectin ternary complex: formation mechanism, emulsion stability, and structure. *J. Sci. Food Agric.* 103 (3), 1442–1453.
- Jiao, Y., Shi, L., Li, D., Chang, Y., 2023. Lutein-loaded glycosylated zein nanoparticles-preparation, characterization, and stability in functional drink. *Lwt-Food Science and Technology* 187.
- Jv, D., Ji, T., Xu, Z., Li, A., Chen, Z., 2023. The remarkable enhancement of photostability and antioxidant protection of lutein coupled with carbon-dot. *Food Chem.* 405.
- Kaur, N., Gupta, A.K., 2004. Importance of inulin-type fructans in health. *AGRO FOOD INDUSTRY HI-TECH* 15 (2), 46–48.
- Khalil, M., Raila, J., Ali, M., Islam, K.M.S., Schenk, R., Krause, J., Schweigert, F.J., Rawel, H., 2012. Stability and bioavailability of lutein ester supplements from tagetes flower prepared under food processing conditions. *J. Funct.Foods* 4 (3), 602–610.
- Krebs, G., Becker, T., Gastl, M., 2017. Characterization of polymeric substance classes in cereal-based beverages using asymmetrical flow field-flow fractionation with a multi-detection system. *Anal. Bioanal. Chem.* 409 (24), 5723–5734.
- Li, L., Chai, W., Ma, L., Zhang, T., Chen, J., Zhang, J., Wu, X., 2023. Covalent polyphenol with soybean 11s protein to develop hypoallergenic conjugates for potential immunotherapy. *J. Funct.Foods* 104.
- Li, Y., Zhou, L., Zhang, H., Liu, G., Qin, X., 2023. Preparation, characterization and antioxidant activity of glycosylated whey protein isolate/proanthocyanidin compounds. *Foods* 12 (11).
- Liu, J., Song, G., Zhou, L., Yuan, Y., Wang, D., Yuan, T., Li, L., He, G., Xiao, G., Chen, F., Gong, J., 2023. Sonochemical effects on fabrication, characterization and antioxidant activities of beta-lactoglobulin-chlorogenic acid conjugates. *Ultrason. Sonochem.* 92.
- Mohammadi, A., Kashi, P.A., Kashiri, M., Bagheri, A., Chen, J., Ettelaie, R., Jager, H., Shahbazi, M., 2023. Self-assembly of plant polyphenols-grafted soy proteins to manufacture a highly stable antioxidative pickering emulsion gel for direct-ink-write 3d printing. *Food Hydrocolloids* 142.
- Moller, M., Denicola, A., 2002. Protein tryptophan accessibility studied by fluorescence quenching. *Biochem. Mol. Biol. Educ.* 30 (3), 175–178.
- Mora-Gutierrez, A., Marquez, S.A., Attaie, R., de Gonzalez, M.T.N., Jung, Y., Woldesenbet, S., Moussavi, M., 2022. Mixed biopolymer systems based on bovine and caprine caseins, yeast beta-glucan, and maltodextrin for microencapsulating lutein dispersed in emulsified lipid carriers. *Polymers* 14 (13).
- Mori, T., Ishii, T., Akagawa, M., Nakamura, Y., Nakayama, T., 2010. Covalent binding of tea catechins to protein thiols: the relationship between stability and electrophilic reactivity. *Biosc. Biotech. Biochem.* 74 (12), 2451–2456.
- Qi, X., Xu, D., Zhu, J., Wang, S., Peng, J., Gao, W., Cao, Y., 2021. Studying the interaction mechanism between bovine serum albumin and lutein dipalmitate: multi-spectroscopic and molecular docking techniques. *Food Hydrocolloids* 113, 106513.
- Song, F., Tang, D., Wang, X., Wang, Y., 2011. Biodegradable soy protein isolate-based materials: a review. *Biomacromolecules* 12 (10), 3369–3380.
- Song, Z.C., Zhang, H., Niu, P.F., Shi, L.S., Yang, X.Y., Meng, Y.H., Wang, X.Y., Gong, T., Guo, Y.R., 2023. Fabrication of a novel antioxidant emulsifier through tuning the molecular interaction between soy protein isolates and young apple polyphenols. *Food Chem.* 420.
- Sonu, Haider S., Kumari, S., Aggrawal, R., Aswal, V.K., Saha, S.K., 2017. Study on interactions of cationic gemini surfactants with folded and unfolded bovine serum albumin: effect of spacer group of surfactants. *J. Mol. Liq.* 243, 369–379.
- Su, J., Guo, Q., Chen, Y., Mao, L., Gao, Y., Yuan, F., 2020. Utilization of β -lactoglobulin-(–)-epigallocatechin-3-gallate(egcg) composite colloidal nanoparticles as stabilizers for lutein pickering emulsion. *Food Hydrocolloids* 98, 105293.
- Tian, L., Yang, K.J., Zhang, S.L., Yi, J.H., Zhu, Z.B., Decker, E.A., McClements, D.J., 2021. Impact of tea polyphenols on the stability of oil-in-water emulsions coated by whey proteins. *Food Chem.* 343.
- Wang, X., Wang, S., Xu, D., Peng, J., Gao, W., Cao, Y., 2022. The effect of glycosylated soy protein isolate on the stability of lutein and their interaction characteristics. *Front. Nutr.* 9.
- Wen, Q., Ding, Z.Y., Kou, F.S., Zhou, P., 2014. Research and application of s-4800 scanning electron microscope in modern testing and analysis technology. *MECHANICAL COMPONENTS AND CONTROL ENGINEERING III* 668–669, 936–939.
- Xu, D., Aihemaiti, Z., Cao, Y., Teng, C., Li, X., 2016. Physicochemical stability, microrheological properties and microstructure of lutein emulsions stabilized by multilayer membranes consisting of whey protein isolate, flaxseed gum and chitosan. *Food Chem.* 202, 156–164.
- Xu, Y., Li, X., Dai, Z., Zhang, Z., Feng, L., Nie, M., Liu, C., Li, D., Zhang, M., 2023. Study on the relationship between lutein bioaccessibility and in vitro lipid digestion of nanostructured lipid carriers with different interface structures. *Food Hydrocolloids* 139.
- Yan, Y., Zhu, Q., Diao, C., Wang, J., Wu, Z., Wang, H., 2020a. Enhanced physicochemical stability of lutein-enriched emulsions by polyphenol-protein-polysaccharide conjugates and fat-soluble antioxidant. *Food Hydrocolloids* 101.
- Yan, Y., Zhu, Q., Diao, C., Wang, J., Wu, Z., Wang, H., 2020b. Enhanced physicochemical stability of lutein-enriched emulsions by polyphenol-protein-polysaccharide conjugates and fat-soluble antioxidant. *Food Hydrocolloids* 101, 105447.
- Yi, J., Fan, Y., Yokoyama, W., Zhang, Y., Zhao, L., 2016. Characterization of milk proteins-lutein complexes and the impact on lutein chemical stability. *Food Chem.* 200, 91–97.
- Zhang, H., Qi, R., Mine, Y., 2019. The impact of oolong and black tea polyphenols on human health. *Food Biosci.* 29, 55–61.
- Zhao, Z., Poojary, M.M., Skibsted, L.H., Lund, M.N., 2020. Cleavage of disulfide bonds in cystine by uv-b illumination mediated by tryptophan or tyrosine as photosensitizers. *J. Agric. Food Chem.* 68 (25), 6900–6909.
- Zheng, Q., Cai, B., Chen, D., Yu, W.H., Wang, Y.H., Huang, Z.X., 2003. The reaction of metallothionein-3 with dtmb. *Chem. Lett.* 32 (7), 616–617.
- Zhou, H., Bie, S., Li, J., Yuan, L., Zhou, L., 2023. Comparison on inhibitory effect and mechanism of inhibitors on sppo and mppo purified from lijiang snow peach by combining multispectroscopic analysis, molecular docking and molecular dynamics simulation. *Food Chem.* 400.